



Simultaneous measurements of urban and rural particles in Beijing – Part 1: Chemical composition and mixing state

Yang Chen¹, Jing Cai², Zhichao Wang¹, Chao Peng¹, Xiaojiang Yao¹, Mi Tian¹, Yiqun Han², Guangming Shi^{1,3}, Zongbo Shi⁴, Yue Liu², Xi Yang², Mei Zheng², Tong Zhu², Kebin He⁵, Qiang Zhang⁶, and Fumo Yang^{3,1}

¹Center for the Atmospheric Environment Research, Chongqing Institute of Green and Intelligent Technology, Chinese Academy of Sciences, Chongqing 400714, China

²SKL-ESPC and BIC-ESAT, College of Environmental Sciences and Engineering, Peking University, Beijing 100871, China

³Department of Environmental Science and Engineering, College of Architecture and Environment, Sichuan University, Chengdu 610065, China

⁴School of Geography, Earth and Environmental Sciences, University of Birmingham, Birmingham B15 2TT, UK

⁵School of Environment, Tsinghua University, Beijing 100084, China

⁶Department of Earth System Science, Tsinghua University, Beijing, China

Correspondence: Fumo Yang (fmyang@scu.edu.cn) and Mei Zheng (mzheng@pku.edu.cn)

Received: 22 October 2019 – Discussion started: 9 January 2020

Revised: 25 June 2020 – Accepted: 29 June 2020 – Published: 5 August 2020

Abstract. Two single-particle aerosol mass spectrometers (SPAMs) were deployed simultaneously at an urban and a rural site in Beijing during an intensive field campaign from 1 to 29 November 2016 to investigate the source and process of airborne particles in Beijing. In the first part of this research, we report the single-particle chemical composition, mixing state, and evolution at both sites. A total of 96 % and 98 % of collected particles were carbonaceous at the urban and rural sites, respectively. Five particle categories, including elemental carbon (EC), organic carbon (OC), internal-mixed EC and OC (ECOC), potassium-rich (K-rich), and metals, were observed at both sites. The categories were partitioned into particle types depending on different atmospheric processing stages. A total of 17 particle types were shared at both sites. In the urban area, nitrate-containing particle types, such as EC-Nit (Nit: nitrate) and ECOC-Nit, were enriched especially at night, sulfate-containing particles were transported when wind speed was high, and ECOC-Nit-Sul (Sul: sulfate) were mostly aged locally. In sum, these processed particles added up to 85.3 % in the urban areas. In the rural area, regional particles were abundant, but freshly emitted ECOC and OC had distinct patterns that were pronounced at cooking and heating times. Biomass burning, traffic, and coal burning were major sources of particulate matter (PM_{2.5}) in both rural and urban areas. Moreover, particles from the steel

industry located in the south were also identified. In summary, the chemical composition of urban and rural particle types was similar in Beijing; the urban particles were influenced significantly by rural processing and transport. The work is useful to understand the evolution of urban and rural particles in Beijing during winter.

1 Introduction

China has experienced severe haze events caused by extremely high concentrations of fine particulate matter (PM_{2.5}) since January 2013. In the worst cases, an area of 2.0 million km² and a population of 800 million were affected (Huang et al., 2014). In the Beijing–Tianjin–Hebei (BTH) area, extreme haze events frequently occur during winter, with PM_{2.5} mass rapidly reaching up to 200 μg m⁻³ and such levels being sustained for hours (Guo et al., 2014).

Over the last 2 decades, comprehensive studies have been conducted on urban PM in Beijing. He et al. (2001) reported the first characterization of PM_{2.5}. Since then, numerous studies have been published on the characterization (Huang et al., 2010), sources (Guo et al., 2012; Sun et al., 2014a), and processing of PM (Sun et al., 2013). The mechanism of rapid-boosting PM_{2.5} in Beijing, including new particle for-

mation and growth (Guo et al., 2014), regional transport (Li et al., 2015a), and both (Du et al., 2017; Sun et al., 2014a), have been proposed. However, discrepancies remain among these studies. For example, the mass loading of PM_{2.5} can rapidly increase to hundreds of micrograms per cubic meter ($\mu\text{g m}^{-3}$). Both Wang et al. (2016b) and Cheng et al. (2016) suggested the secondary formation of sulfate from the oxidation of NO₂, while Guo et al. (2014) have proposed a mechanism of particle formation and growth. Different from local secondary formation and accumulation, Li et al. (2015b) proposed that particles via long-range transport cause the elevation of PM_{2.5}. According to Sun et al. (2014b) and Zhai et al. (2018), regional transport played important roles during heavy haze episodes. However, most of the studies have focused on the urban areas of Beijing with limited attention to the rural areas. To illustrate the sources, evolution, and transport of particles, the investigation of rural areas around Beijing is necessary.

Single-particle mass spectrometers (SPMSs) have been used to investigate the size-resolved chemical composition and mixing state of atmospheric particles (Gard et al., 1997; Pratt and Prather, 2012). More recently, single-particle aerosol mass spectrometers (SPAMSs) have been used in Chinese megacities such as Beijing (Li et al., 2014), Shanghai (Tao et al., 2011), Guangzhou (Bi et al., 2011), Xi'an (Chen et al., 2016), Nanjing (Wang et al., 2015), and Chongqing (Chen et al., 2017). SPAMS has proven to be a useful tool for characterizing the single-particle chemical composition, mixing state, and processing of atmospheric particles. Due to the nature of laser desorption ionization (LDI), the instrument is very sensitive to dust and other types of particles containing sodium and potassium. This may cause bias in the particle matrix (Pratt and Prather, 2012).

In Beijing, particle types, such as carbonaceous, metallic, dust, potassium-rich, and others, were reported during spring and fall (L. Liu et al., 2016; Li et al., 2014). Moreover, lead-containing particles have also been investigated in recent studies (Ma et al., 2016; Cai et al., 2017). Organics, sulfate, nitrate, ammonium, and other species have been found internally mixed with the atmospheric particles, and these particle types are mostly from the combustion of fuel or biomass. The abundance of secondary species can indicate the degree of aging during atmospheric processing. Particles are mostly secondary species with deeper processing. However, these studies lack the use of these data to provide a view of dynamic particulate processing. These studies have focused on the urban areas of Beijing, limiting their information to the characterization of the particles in the Beijing region. Therefore, a simultaneous study to investigate the particle chemical composition and mixing state would fill the gap.

This study is part of the APHH-Beijing (Air Pollution and Human Health in a Chinese Megacity: Beijing) intensive field campaign during winter 2016 (Shi et al., 2019). Two SPAMSs were deployed simultaneously at Peking University

(PKU) and Pinggu (PG) in order to observe both urban and rural particles in the Beijing region. The aims of the study are (1) to characterize the single-particle chemical composition and mixing state and (2) to investigate particulate evolution and mixing state during haze events. These two objectives are presented in two parts. In Part 1, particle types and their atmospheric processing (e.g., origination, source, and diurnal profiles) at both sites are reported; in Part 2 (Chen et al., 2020), the detailed analysis of haze events, effects of heating activities, and evidence of regional transport are addressed.

2 Methodology

2.1 Sampling sites

The campaigns were performed simultaneously at PKU (39.99° N, 116.32° E) and PG (40.17° N, 117.05° E) from 1 to 29 November 2016. A Description of the PKU site is available in the literature (Huang et al., 2006). Briefly, the site is located on a rooftop (15 m above the ground) of the PKU campus which is surrounded by residential and commercial blocks. Trace gases including NO, NO₂, SO₂, O₃, and CO (Thermo Inc. series models 42*i*, 43*i*, 49*i*, and 48*i*, respectively), meteorological parameters (Vaisala Inc.), and PM_{2.5} (TEOM 1430) were recorded during the observation.

The PG site (40.173° N, 117.053° E) is 3 km from the PG center. The site is located to the northeast of the PKU site at a distance of 70 km. The PG site also acts as a host of the AIR-LESS (effects of air pollution on cardiopulmonary disease in urban and peri-urban residents in Beijing) Project. The meteorological data are acquired from the local meteorological office. The PG village is surrounded by orchards and farmland with no main road nearby on a scale of 3 km. Coal and biomass are used for domestic heating and cooking in the nearby villages.

2.2 Instrumentation and data analysis

Two SPAMSs (model 0515, Hexin Inc., Guangzhou, China) were deployed at both PKU and PG. A technical description of SPAMS is available in Li et al. (2011). Briefly, a SPAMS has three functional parts: sampling, sizing, and mass spectrometry. In the sampling part, particles within a 0.1–2.0 μm size range pass efficiently through an aerodynamic lens. In the sizing unit, the aerodynamic diameter (D_{va}) is calculated using the time of flight of particles. The particles are then decomposed and individually ionized into ions using a 266 nm laser. A bipolar time-of-flight mass spectrometer measures the ions and generates the positive and negative mass spectra of each particle. The two instruments were maintained and calibrated following the standard procedures before sampling (Chen et al., 2017).

A neural network algorithm based on adaptive resonance theory (ART-2a) was used to resolve particle types from both datasets (Song et al., 1999). The parameters used were as fol-

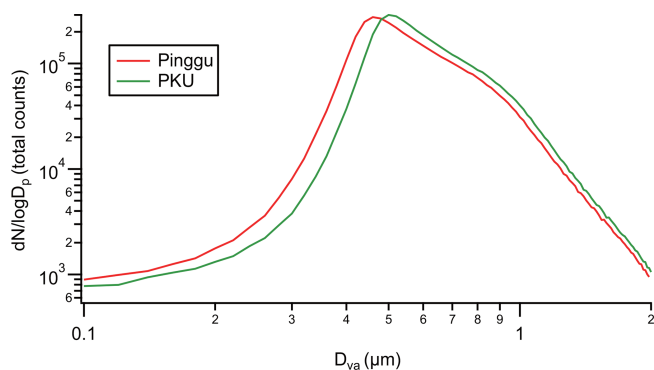


Figure 1. The size distribution of SPAMS particles at PKU and PG sites.

lows: a vigilance factor of 0.70, a learning rate of 0.05, and 20 iterations. This procedure generated 771 and 792 particle groups. Then, the groups were combined into particle types based on similar mass spectra, temporal trends, and size distributions (Dallosto and Harrison, 2006). During combining, relative areas of nitrate and sulfate were used to distinguish between the stages of processing, assuming that more sulfate and nitrate can be measured if a particle is more processed during its lifetime. Thus, particles with relative peak areas of sulfate and nitrate larger than 0.1 were marked with sulfate (-Sul) or nitrate (-Nit), respectively, or both. Indeed, the matrix effect can affect ionic intensities between different particles during single-particle mass spectrometer analysis. However, the effect can be reduced using average mass spectra of particles within the similar size distribution and chemical composition. Finally, the strategy resulted in 20 and 19 particle types at PKU and PG, respectively. Among them, 17 types appeared at both sites, and the same type at both locations had the same mass spectra ($R^2 > 0.80$).

3 Results

A total of 4 499 606 and 4 063 522 particles were collected at the PKU and PG sites, respectively. The size distributions peaked at 0.48 and 0.52 μm (Fig. 1). The smaller size distribution was due to a more substantial fraction of freshly emitted particles at PG, as described in Table 1. A total of 17 particle types ($R^2 > 0.80$, mass spectra) were observed both at PKU and PG (Table 1). These particle types were labeled with the suffixes “_PKU” or “_PG” to indicate their locations. The term “particle category” stands for a group of particle types with variable stages of processing.

3.1 Meteorological conditions and overview

Temperature, relative humidity (RH), and wind speed at both sites during the sampling period are summarized in Table 2. Their temporal trends are available in Part 2. The average temperature at PKU (urban, 5.7 ± 2.3 $^{\circ}\text{C}$) was higher than

at PG (rural, 3.1 ± 2.2 $^{\circ}\text{C}$). Correspondingly, relative humidity was higher at PG (67 ± 32 %) than at PKU (49 ± 30 %). The wind was stronger at PKU (2.5 ± 1.8 m s^{-1}) than at PG (1.7 ± 0.9 m s^{-1}). As shown in Fig. 2, wind speed at PKU peaked at 12:00 LT (local time, UTC+8; hereafter all times are local time), while wind speed at PG reached its maximum at 15:00. Various wind speeds determined the different dispersion patterns of pollutants near the surface. It should be noted that wind speed up to 2 m s^{-1} represents a scale of 172 km in diurnal transport. Therefore, at PKU, the wind could bring the pollutants from Hebei province under stagnant air conditions.

3.2 Common particle categories at both PKU and PG

3.2.1 Elemental carbon category

As shown in Fig. 3a, the elemental carbon (EC) particle category was represented by ions peaking at m/z 12, 24, 36, 48, and 60 in positive mass spectra (Sodeman et al., 2005; Toner et al., 2008). EC is emitted from solid fuel combustion, traffic (Sodeman et al., 2005; Toner et al., 2008, 2006), and industrial activities (Healy et al., 2012). Due to the various ionic intensities of nitrate (m/z -46 and -62) and sulfate (m/z -80 and -97), the EC category has four types including EC-Nitrate (EC-Nit), EC-Sulfate (EC-Sul), and EC-Nit-Sul. Moreover, the EC category was more abundant after the heating began than before (Part 2), indicating that coal burning was one of the primary sources.

EC-Nit_PKU and EC-Nit_PG accounted for 7.0 % and 2.0 % in PKU and PG datasets, respectively. In the diurnal profiles of EC-Nit_PKU, there was an apparent early morning peak at 05:00 along with an evening peak (22:00). There was also an early morning NO_x peak in the urban area of Beijing, providing sufficient precursors for secondary nitrate (Shi et al., 2019). Wang et al. (2018) validated the role of N_2O_5 uptake on the nitrate formation in PM. Therefore, the early morning peak of EC-Nit_PKU occurred due to the uptake of nitrate on the freshly emitted EC in the early morning (Sun et al., 2014a). The evening peak could be due to the low temperature after the heating supply started (D. Liu et al., 2019). Diurnally, EC-Nit_PG exhibited an early morning peak (05:00) but no evening peak and mainly came from the southeast.

EC-Nit-Sul was more abundant at the rural site (18.6 %) than the urban site (11.6 %). EC-Nit-Sul_PKU (10.5 %) had early morning (04:00), morning (07:00), and afternoon (around 16:00) peaks, while EC-Nit-Sul_PG (3.5 %) had early morning (04:00), noon, and afternoon (17:00, Fig. 3a) peaks. However, they showed relatively small diurnal variations. For example, EC-Nit-Sul_PKU varied between 800 and 1000 count h^{-1} , and EC-Nit-Sul_PG shifted between 200 and 250 count h^{-1} . Thus, the EC-Nit-Sul at both sites was most likely acting as background and regional particles (Dall’Osto et al., 2016). Additionally, EC-Nit-Sul_PKU

Table 1. SPAMS particle types identified at the PKU and PG sites.

Particle type	PKU number	PKU percentage	PG number	PG percentage	Comments
EC-Nit	313 574	7.0	79 082	2.0	Solid fuel burning, traffic
EC-Nit-Sul	473 908	10.5	140 107	3.5	
EC-Sul	30 365	0.7	4096	0.1	
ECOC-Nit-Sul	539 533	12.0	755 279	18.6	Traffic, coal burning
ECOC-Sul	572 548	12.7	397 367	9.8	
K-rich	322 731	7.2	259 287	6.4	Aged biomass burning
K-Nit	359 281	8.0	334 547	8.2	
K-Nit-Sul	717 280	16.0	76 954	1.9	
K-Sul	26 301	0.6	183 571	4.5	
NaK	16 680	0.4	74943	1.8	Coal, peat
NaK-Nit	289 259	6.4	697 60	1.7	
NaK-Nit-Sul	114 387	2.5	77 555	1.9	
NaK-Sul	7509	0.2	16 578	0.4	
OC-Nit-Sul	334 870	7.4	865 821	21.3	Traffic, coal burning
OC-Sul	40 800	0.9	279 322	6.9	
Ca-dust	19 869	0.4	3035	0.1	Dust
Fe-rich	137 600	3.1	70 920	1.8	Steel industry
ECOC-Nit	137 470	3.1 %			Solid fuel burning
OC-Nit	41 159	0.9 %			Traffic, coal burning
K-Amine-Nit-Sul	4482	0.1 %			Coal burning
ECOC			239 953	5.9 %	Coal burning
OC			135 345	3.3 %	Traffic, coal burning

Note: Nit stands for nitrate and Sul for sulfate.

Table 2. Meteorological parameters at PKU and PG during the campaign.

	PKU	PG
Temperature (°C)	5.7 ± 2.3	3.1 ± 2.2
RH (%)	49 ± 30	67 ± 32
Wind speed (m s ⁻¹)	2.5 ± 1.8	1.7 ± 0.9

mainly came from the surrounding areas of the city in a pollution plume, while EC-Nit-Sul_PG mainly came from the southeast (Fig. 3c).

EC-Sul was a minor type at both sites, accounting for 0.7 % at PKU and 0.1 % at PG. EC-Sul was pronounced in the afternoon when the wind was strong at both sites. It was unlikely for either EC-Sul_PKU or EC-Sul_PG to be local because their concentrations were associated with high wind speed, as shown in Fig. 3c. More specifically, EC-Sul_PKU came from the southeast and northeast of Hebei Province when the wind speed exceeded 6 m s⁻¹. EC-Sul_PG could have come from the west when the wind speed exceeded

2 m s⁻¹ and the east when the wind speed exceeded 3 m s⁻¹ as coal-using industries are located in both directions. Also, at both sites, the concentrations of SO₂ were elevated in the afternoon due to transport, providing sufficient precursors for the formation of sulfate (Shi et al., 2019).

3.2.2 Organic carbon category

The positive mass spectra of both OC-Nit (OC: organic carbon) and OC-Nit-Sul contained complicated organic ions such as C₂H₃⁺ (*m/z* 27), C₃H⁺ (*m/z* 37), C₃H₇⁺/C₂H₃O⁺/CHNO⁺ (*m/z* 43), C₄H₂⁺ (*m/z* 50), aromatic hydrocarbons (C₄H₃⁺, C₅H₃⁺, and C₆H₅⁺), and diethylamine ((C₂H₅)₂NH₂⁺, *m/z* 74, and (C₂H₅)₂NCH₂⁺, *m/z* 86). The negative mass spectra contained CN⁻ (*m/z* -26), Cl⁻ (*m/z* -35 and 37), CNO⁻ (*m/z* -42), nitrate (*m/z* -46 and -62), and sulfate (*m/z* -97). The presence of CN⁻ and CNO⁻ suggests the existence of organonitrogen species (Day et al., 2010). Peak intensities of organic fragments are relatively high in the OC-Sul particles, indicating that it was relatively fresh, while OC-Nit-Sul was more

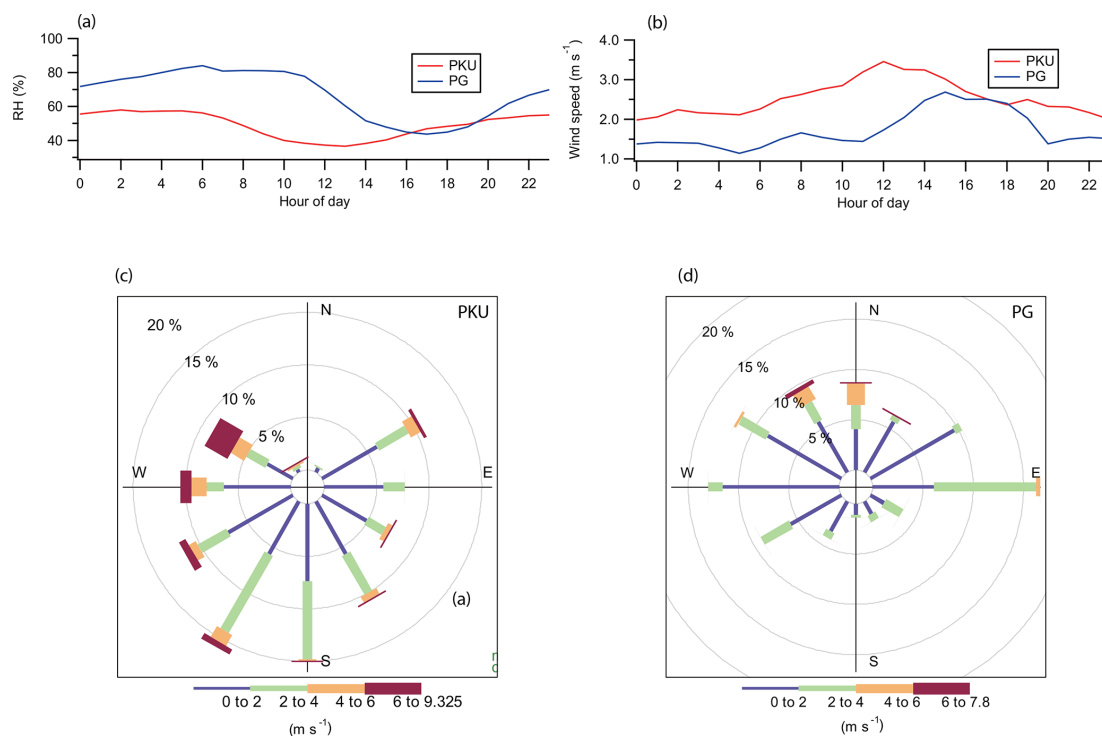


Figure 2. Diurnal plots of (a) RH and (b) wind speed; rose plots of wind at (c) PKU and (d) PG.

processed (Zhai et al., 2015; Peng et al., 2020a). The positive mass spectrum had similar ions of coal combustion organic aerosol (CCOA) with significant signals of polycyclic aromatic hydrocarbons in AMS studies (Sun et al., 2013). OC-Sul showed different spatial distributions with 0.9 % at PKU and 6.9 % at PG.

OC-Sul_PG had morning (08:00) and afternoon (16:00) peaks, while the diurnal profile of OC-Sul_PKU showed a trend with early morning (03:00), morning (10:00), and afternoon (16:00) peaks. The diurnal trends OC-Sul at both PKU and PG were consistent with the heating patterns depending on the variation of local temperature. Moreover, OC-Sul_PG increased after the heating supply began. Polar plots suggest that OC-Sul_PKU came from the surrounding southwestern areas via transport, while OC-Sul_PG came from villages to the east and west (Fig. 4). These results suggest that OC-Sul_PG was emitted from coal burning for residential heating in nearby areas.

OC-Nit-Sul accounted for 7.4 % and 21.3 % of all detected particles at PKU and PG, respectively. OC-Nit-Sul_PKU had a diurnal peak at 07:00 during rush hour, suggesting that OC-Nit-Sul could be formed due to the uptake of nitrate on OC-Sul, while OC-Nit-Sul_PG had a diurnal peak at 08:00 due to traffic in nearby towns. As an aged particle type, OC-Nit-Sul_PKU and OC-Nit-Sul_PG, also acting similar to background types with hourly counts, remained low but had elevated to high levels at night. Polar plots suggest that OC-Nit-Sul_PKU mainly came from the surrounding areas, while

OC-Nit-Sul_PG mainly came from the south and east, where populous villages are located (Fig. 4).

3.2.3 ECOC category

As shown in Fig. 5a, the internal-mixed elemental carbon and organic carbon (ECOC) category contained two major particle types: ECOC-Nit-Sul and ECOC-Sul. The positive mass spectrum of ECOC-Nit-Sul contained C_n^+ (m/z 12, 24, 36...), NH_4^+ (m/z 18), $C_2H_3^+$ (m/z 27), K^+ (m/z 39 and 41), $C_3H_7^+/C_2H_3O^+/CHNO^+$ (m/z 43), $C_4H_2^+$ (m/z 50), and $[(C_2H_5)_2NH_2]^+$ (m/z 74); in the negative mass spectrum, ions such as sulfate (m/z -80 and -97), nitrate (m/z -46 and -62), C_n^- , and CN^- (m/z -26) were abundant. This mixture of EC and OC particle types was common in single-particle studies. ECOC could be local or from incomplete combustion processes (Chen et al., 2017) or from regional transport, e.g., after aging (McGuire et al., 2011; Huang et al., 2013; Zhao et al., 2019). The diurnal profile of ECOC-Sul_PG showed early morning (01:00), morning (08:00), and afternoon (17:00) peaks, which is consistent with local cooking and heating patterns. Also, heating activities enhanced the fraction of ECOC-Sul_PG. ECOC-Sul_PG did not show a clear diurnal profile, suggesting that ECOC-Sul_PG was mainly a background type. Similarly, ECOC-Nit-Sul_PKU and ECOC-Nit-Sul_PG were also background types with less obvious diurnal variations (Dall'Osto et al., 2016). Polar plots (Fig. 5c) suggested that ECOC-Nit-

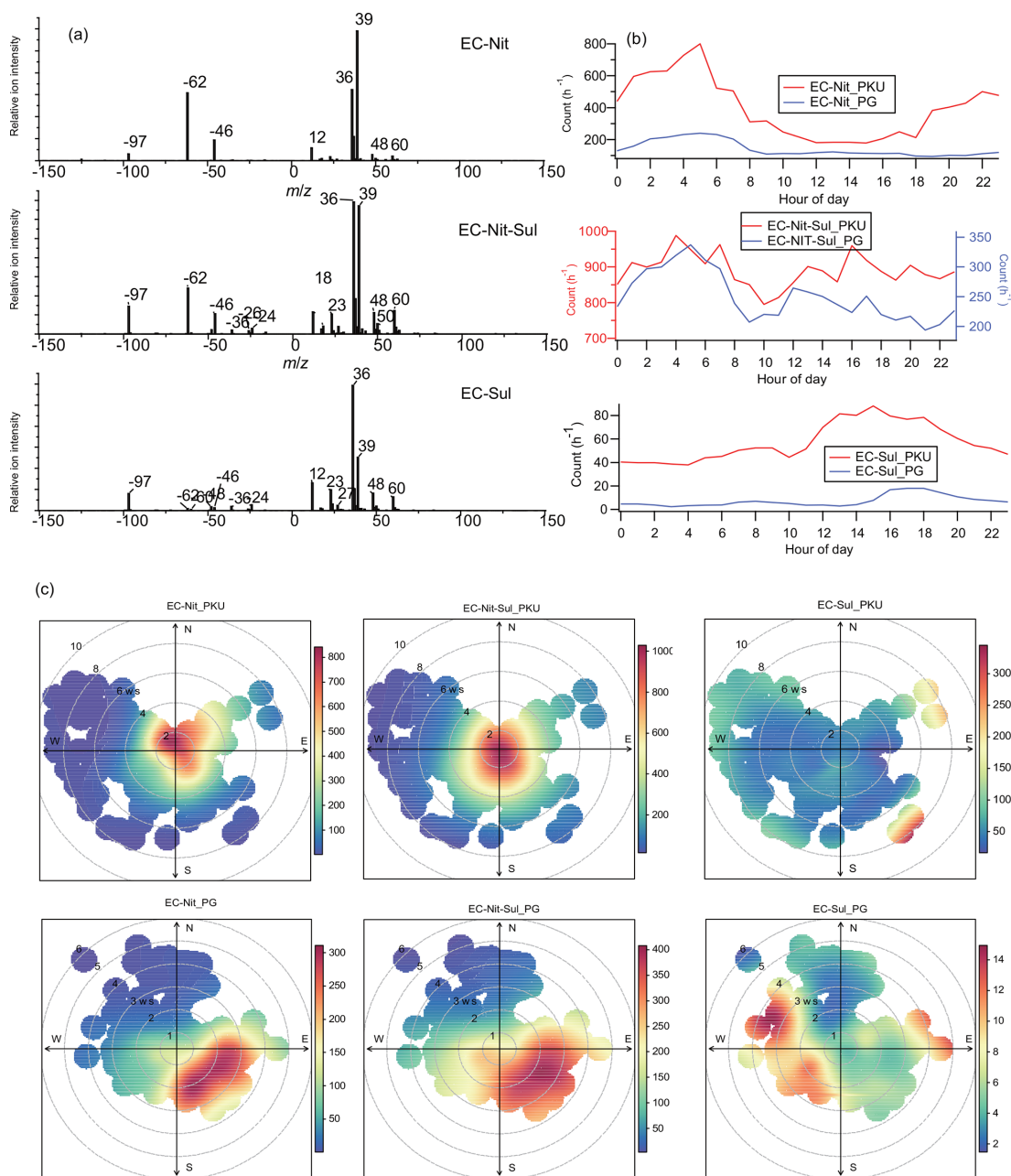


Figure 3. (a) Average mass spectra of EC-Nit, EC-Nit-Sul, and EC-Sul at both sites; (b) diurnal patterns of EC-Nit, EC-Nit-Sul, and EC-Sul at both sites; (c) polar plots of EC-Nit, EC-Nit-Sul, and EC-Sul; the gray circles indicate wind speed (m s^{-1}).

Sul_PKU and ECOC-Sul_PKU had both local and regional sources. Wind speeds up to 4 m s^{-1} could cause a transport at a distance of 346 km diurnally, indicating that it was possible for the particles from Hebei province to have arrived at the sampling place.

3.2.4 Potassium-rich category

Figure 6 shows a series of potassium-rich (K-rich) particle types. The K-rich category contained Na^+ (m/z 23), C_2H_3^+

(m/z 27), C_n^+ , C_3H^+ (m/z 37), K^+ , aromatic hydrocarbons (C_4H_3^+ , C_5H_3^+ , and C_6H_5^+), levoglucosan (m/z -45, -59, and -71), sulfate, and nitrate. According to the ionic intensities of sulfate and nitrate, the K-rich particle category had several branches such as K-rich, K-Nit, K-Sul, and K-Nit-Sul. K-rich particles are commonly found in biomass burning (BB) emissions (Silva et al., 1999; Pagels et al., 2013; Chen et al., 2017). Cl^- was not abundant in all K-rich particle types, suggesting that the K-rich particles had undergone aging during atmospheric processing (Sullivan et al., 2007;

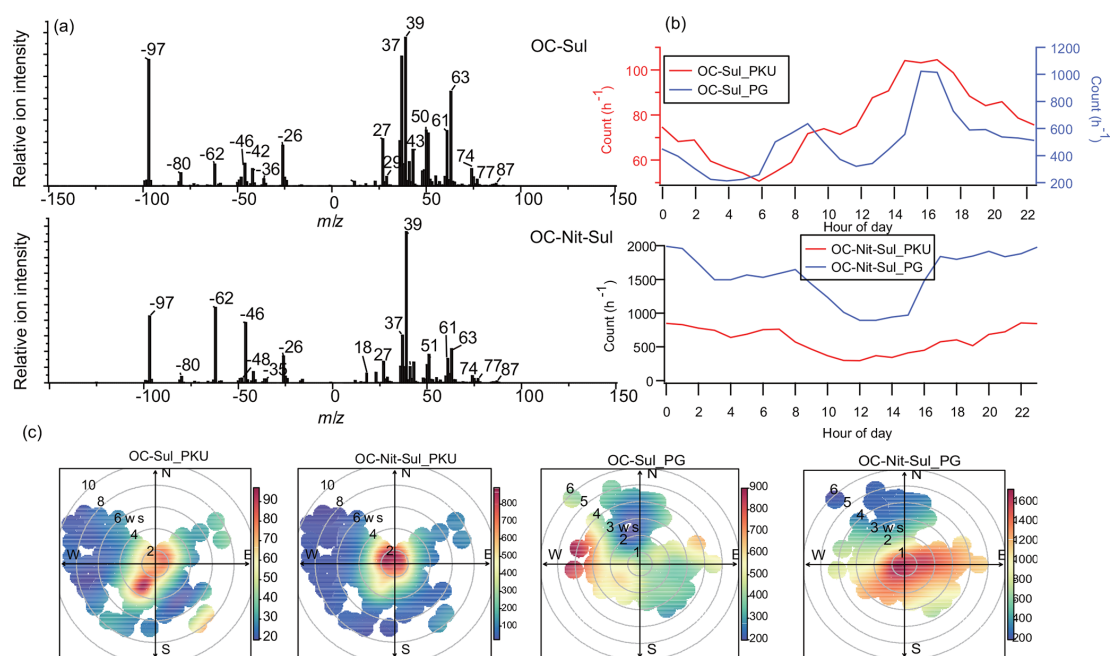


Figure 4. (a) Average mass spectra of OC-Nit and OC-Nit-Sul observed at both sites; (b) diurnal patterns of the hourly count of OC-Nit and OC-Nit-Sul at both sites; (c) polar plots of OC-Sul and OC-Nit-Sul; the gray circles indicate wind speed (m s^{-1}).

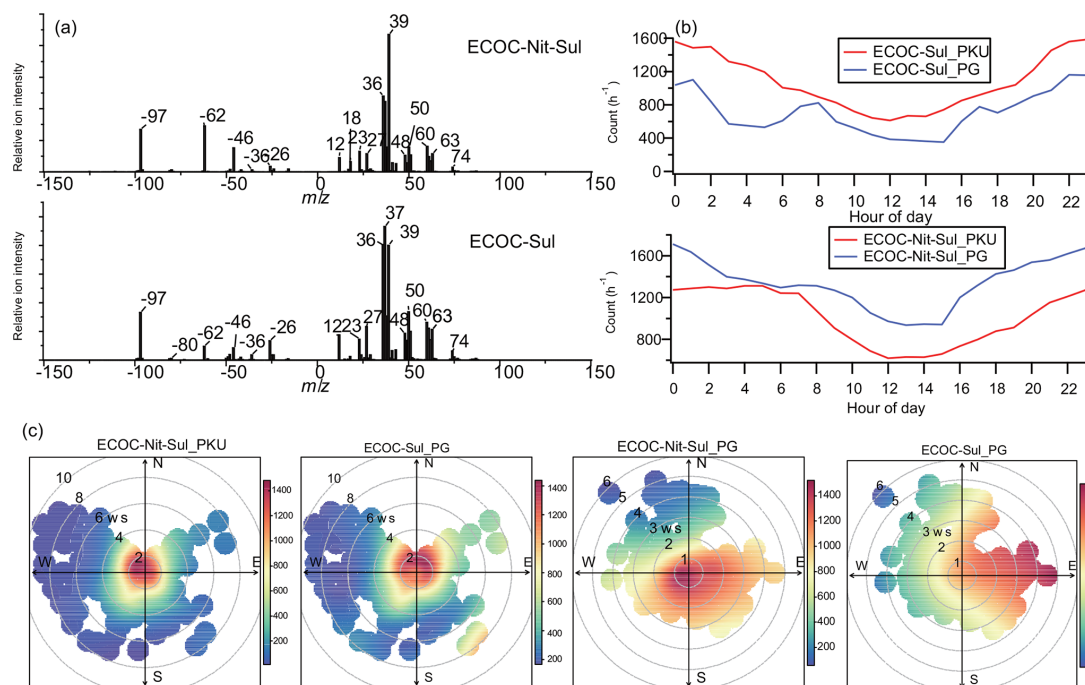


Figure 5. (a) Average mass spectra of ECOC-Nit and ECOC-Nit-Sul observed at both sites; (b) diurnal patterns of the hourly count of ECOC-Sul and ECOC-Nit-Sul at both sites; (c) polar plots of ECOC-Sul and ECOC-Nit-Sul; the gray circles indicate wind speed (m s^{-1}).

Chen et al., 2016), but K-Nit, K-Nit-Sul, and K-Sul were more processed.

All K-rich category particles showed different atmospheric evolution processes at both PKU and PG. K-rich_PKU illustrated a typical pattern that was at low levels in the daytime but high levels at night (22:00). As shown in Fig. 6c, at an average wind speed of 3 m s^{-1} , it took 5 h for particles at a distance of 50 km to arrive at PKU. This is also the reason why BB-related particles were abundant in urban Beijing where household BB is prohibited. The origination of K-rich_PKU was from nearby and the southwest. K-rich_PG, however, showed a pattern with cooking and heating activities, peaking at 07:00 and 17:00. The peak at 07:00 was due to the local emissions; the 17:00 emissions could be transported from a distance of 50 km at a wind speed of 3 m s^{-1} from the east and west.

The secondary process contributed to the early morning peak (05:00) of K-Nit_PKU due to the nighttime formation of nitrate via hydrolysis of N_2O_5 in the NO_x -rich urban areas (Wang et al., 2017). In the daytime, after rush hour, the number concentration of K-Nit_PKU increased again via the uptake of nitrate due to daytime photoactivity. K-Nit_PKU mainly originated from the local and southern areas (Fig. 6c). Besides the early morning peak, K-Nit_PG showed cooking and heating patterns that were abundant when the temperature was low in the early morning and afternoon. K-Nit_PG largely originated from both local and regional sources via long-range transport.

3.2.5 Metal category

Two metal-rich particle types were identified, namely Fe-rich and Ca-rich. The Fe-rich type contained iron (m/z 56 and 54), K^+ , Na^+ , NH_4^+ , Cl^- (m/z -35 and -37), sulfate, and nitrate. The Ca-rich type was composed of Ca^+ (m/z 40), CaO (m/z 56), K^- , Na^+ , Cl^- , sulfate, and nitrate. As shown in Fig. 6b, Ca-rich_PKU (0.4 %) and Ca-rich_PG (0.1 %) were likely of regional origin with no distinct diurnal variations. Since SiO_2^- and SiO_3^- (m/z -60 and -76) were not abundant in the Ca-rich particles, they are not likely to come from dust (Silva et al., 2000). According to its weak peaks during rush hour at PKU, a possible source of the Ca-rich particles was from road dust resuspension. Such rush hour peaks were not observed at PG.

Fe-rich_PKU (3.1 %) and Fe-rich_PG (1.8 %) had similar diurnal profiles that arose in the early morning when heavy-duty vehicles were allowed to enter the 5th Ring expressway. The peak occurred earlier at PG (04:00 rather than 05:00) because these vehicles got closer to PG earlier than to PKU. The daytime peak occurred in the afternoon at both PKU and PG when wind speed was high. Therefore, there were also multiple sources for Fe-rich particles, including resuspended dust particles from traffic and fly ash from the steel industry. In Beijing, daytime Fe-rich particles were reported and assigned to long-range transport and industrial sources from

Hebei Province (Fig. 7c) (Li et al., 2014). The steel industry moved out of Beijing more than a decade ago (L. Liu et al., 2016). Currently, most of these steel industries are located in Hebei Province.

3.2.6 NaK category

As shown in Fig. 8, mass spectra of the NaK category contained Na^+ , K^+ , C_n^+ , C_n^- , nitrate, and PO_3^- (m/z -79). The aged NaK particles contained strong signals of nitrate (NaK-Nit), sulfate (NaK-Sul), or both (NaK-Nit-Sul). In general, the NaK category contained stronger signals of Na^+ than the EC and K-rich categories. The NaK category may also come from incomplete solid fuel combustion processes such as coal, peat, or wood (Chen et al., 2017; Healy et al., 2010; Xu et al., 2017). The NaK category was more abundant at PKU (9.5 %) than PG (5.8 %), suggesting a stronger contribution of emissions from coal boilers (Xu et al., 2017, 2018). Additionally, after heating began, the fraction of NaK-Nit_PG and NaK-Sul-Nit_PG increased by 1.2 times (see Part 2).

NaK_PKU showed no distinct diurnal variations, suggesting that it was a regional particle type arriving at the PKU site via transport, while NaK_PG showed an apparent diurnal variation consistent with cooking and heating patterns. Polar plots also suggest that they are from the east and the west. NaK-Nit, with a considerable uptake of nitrate, was more abundant at PKU (6.4 %) than PG (1.7 %). Both NaK-Nit_PKU and NaK-Nit_PG increased in the afternoon when photochemical activities were most active (Fig. 8c). Both of them may be from regional transport (Fig 8b and c).

NaK-Sul was a minor particle type at both PG and PKU, accounting for 0.2 % and 0.4 %, respectively. The diurnal profile of NaK-Sul_PG was also following the local cooking and heating patterns, while NaK-Sul_PKU showed a typical transport pattern that became abundant in the afternoon as the southwesterly wind speed increased. As a heavily aged particle type, NaK-Nit-Sul was transported to both PKU and PG from the southwest. In short, NaK-related particle types mainly came from the solid fuel burning process, e.g., coal. Due to its different origins, it showed different levels of processing at PKU and PG.

3.3 Unique particle types at the PKU site

OC-Nit_PKU (0.9 %) and ECOC-Nit_PKU (3.1 %) with strong ion intensities of nitrate were observed at the PKU site. OC-Nit_PKU and ECOC-Nit_PKU showed a peak at nighttime rather than at daytime, similar to the diurnal profiles of OC-Nit-Sul_PKU and ECOC-Nit-Sul_PKU. Such nitrate-rich particle types could have come from the uptake of nitrate in OC and ECOC (Qin et al., 2012; Chen et al., 2016). Polar plots suggest that both types were formed locally when the wind speed was lower than 4 m s^{-1} . The NO_x -rich environment in urban Beijing provides a favorable condition

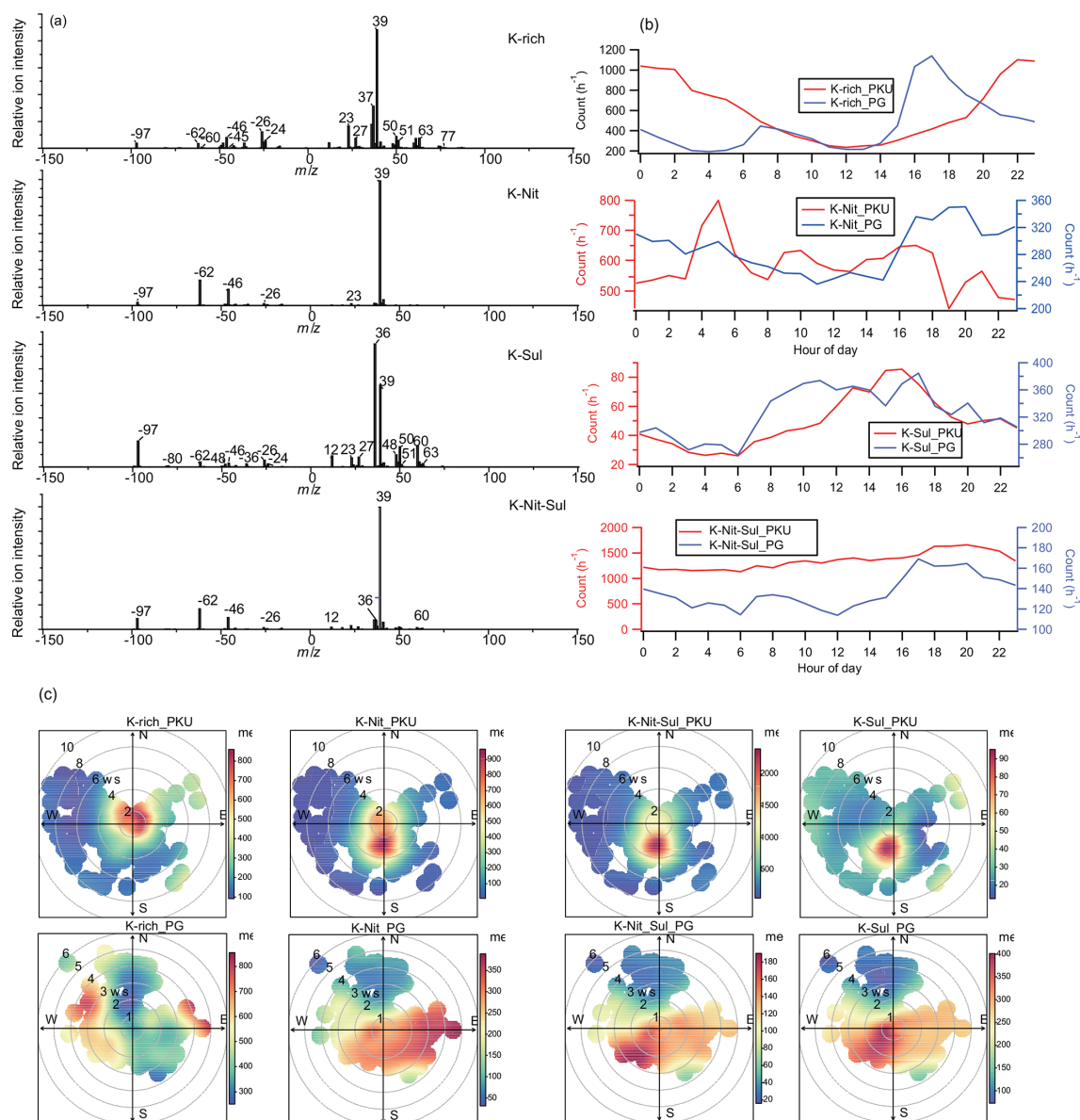


Figure 6. (a) Average mass spectra of BB, K-Nit, K-Sul, and K-Nit-Sul observed at both sites; (b) diurnal patterns of the hourly count of K-rich, K-Nit, K-Sul, and K-Nit-Sul at both sites; (c) polar plots of BB, K-Nit, K-Sul, and K-Nit-Sul; the gray circles indicate wind speed (m s^{-1}).

for nitrate formation at night (Wang et al., 2016a; Zou et al., 2015; Shi et al., 2019).

A minor amount (0.10 %) of amine-containing particles were observed at the PKU site, and trimethylamine ion fragments (m/z 58 and 59) were influential in the mass spectrum of K-amine-Nit-Sul_{PKU} (Fig. 9a). The diurnal profile of K-amine-Nit-Sul_{PKU} showed an afternoon peak, indicating a regional source (Fig. 9c). K-amine-Nit-Sul_{PKU} was transported to the site from nearby locations. The amines may come from animal husbandry, BB, traffic, or vegetation (Chen et al., 2019). Amines were ubiquitous in the atmospheric environment, playing essential roles in new particle

formation and growth, as well as fog and cloud processing (Ge et al., 2011; Chen et al., 2019).

3.4 Unique particle types at the PG site

OC_{PG} (5.9 %) and ECOC_{PG} (3.3 %) were only observed at the rural PG site (Fig. 10). The major components of these two types were consistent with the OC and ECOC categories but with limited uptake of sulfate and nitrate, respectively, suggesting that they were possibly freshly emitted particles (Peng et al., 2020b). Their diurnal profiles are consistent with cooking and heating patterns which peaked at 07:00 in the

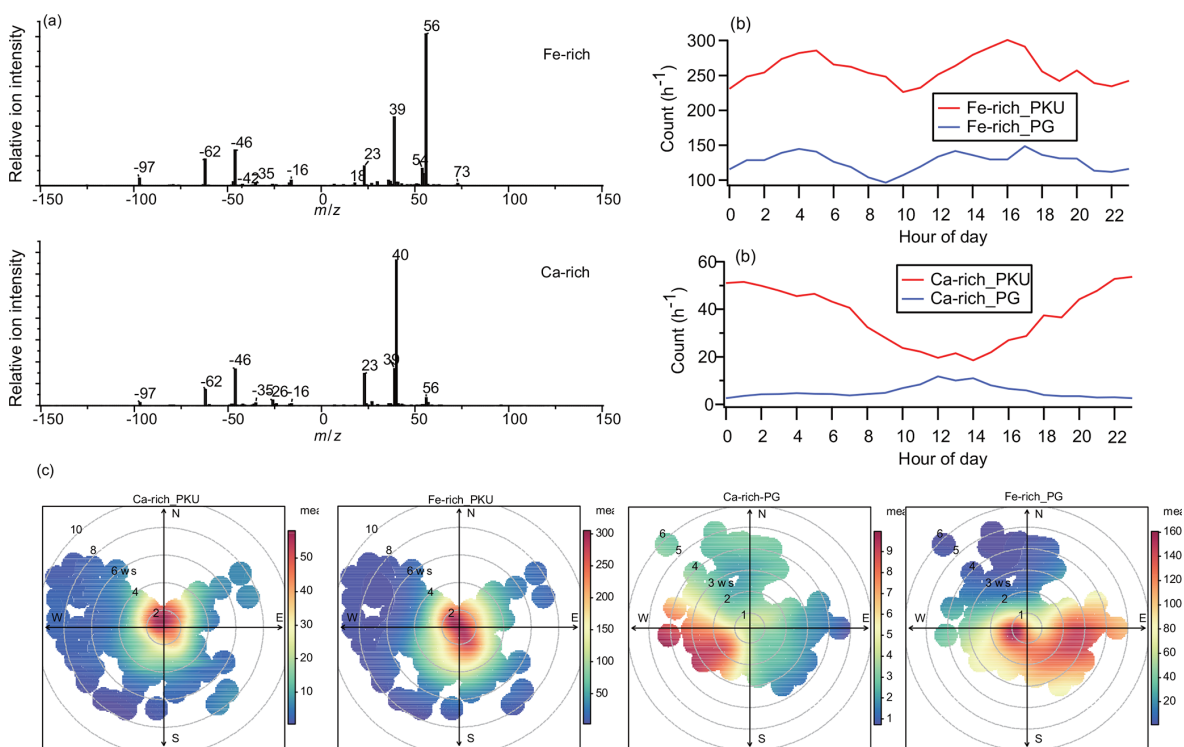


Figure 7. (a) Average mass spectra of Fe-rich and Ca-rich observed at both sites; (b) diurnal patterns of the hourly count of Fe-rich and Ca-rich types at both sites; (c) polar plots of Fe-rich and Ca-rich types; the gray circles indicate wind speed (m s^{-1}).

morning and 17:00. Polar plots suggest that OC_PG mainly came from nearby and from other remote areas in all directions except the north. ECOC mainly came from the east of the PG site. These results support the assumption that the two types were mainly from local emission sources. Also, the emission of OC_PG and ECOC_PG is prevalent in the region.

4 Discussion

Multiple models for source apportionment have been used in Beijing to quantify the sources of particles (Sun et al., 2014a; Xu et al., 2015; Zhai et al., 2018). Biomass burning, coal combustion, traffic, and dust are the key sources of PM (Sun et al., 2014a; Liu et al., 2018; Huang et al., 2014). Multiple studies have confirmed that biomass burning is an essential source of PM in urban Beijing (Gao et al., 2014; Huang et al., 2014; Sun et al., 2014a; Zheng et al., 2017). In this study, biomass burning and other solid fuel burning were identified as crucial sources of PM in not only urban but also rural areas of Beijing. We observed that BB-related particles (K-rich category) were more abundant at PG than at PKU. In particular, we found freshly emitted K-containing particles at the Pinggu site, confirming the importance of local emissions to PM. Furthermore, K-containing particles in the urban area were more aged, suggesting that they are aged mostly from

the surrounding areas. This result is consistent with that of Y. Liu et al. (2019) based on combined receptor and footprint models. Nevertheless, household emissions in the BTH region caused 32 % and 15 % of primary $\text{PM}_{2.5}$ and SO_2 . These studies have proven the importance of household emissions from BB in the BTH area (J. Liu et al., 2016). Especially at the PG site, the ambient PM was mainly controlled by long-range transport and household emissions from cooking and heating.

Due to the nature of SPAMS, the chemical composition of PM cannot be precisely quantified. However, single-particle aerosol mass spectrometers have advantages in studying the chemical composition, mixing state, source, and process of particles (Pratt and Prather, 2012). Mass-based technologies can not differentiate between the origins of the bulk of nitrate or whether it is transported or formed locally. Indeed, single-particle types in urban Beijing have been reported in previous studies (Li et al., 2014; L. Liu et al., 2016), and the major types are consistent with this study. However, in this study, we adopted a cluster strategy considering the relative ion peak area of sulfate and nitrate as indicators of particle processing. Therefore, more detail could be extracted from both datasets. We confirmed that the source, origin, and processes were different for these particles in the urban and rural areas. For example, the seriously processed particles, such as K-Nit-Sul, OC-Nit-Sul, and NaK-Nit-Sul, acted with no distinct diurnal patterns as background or regional sources

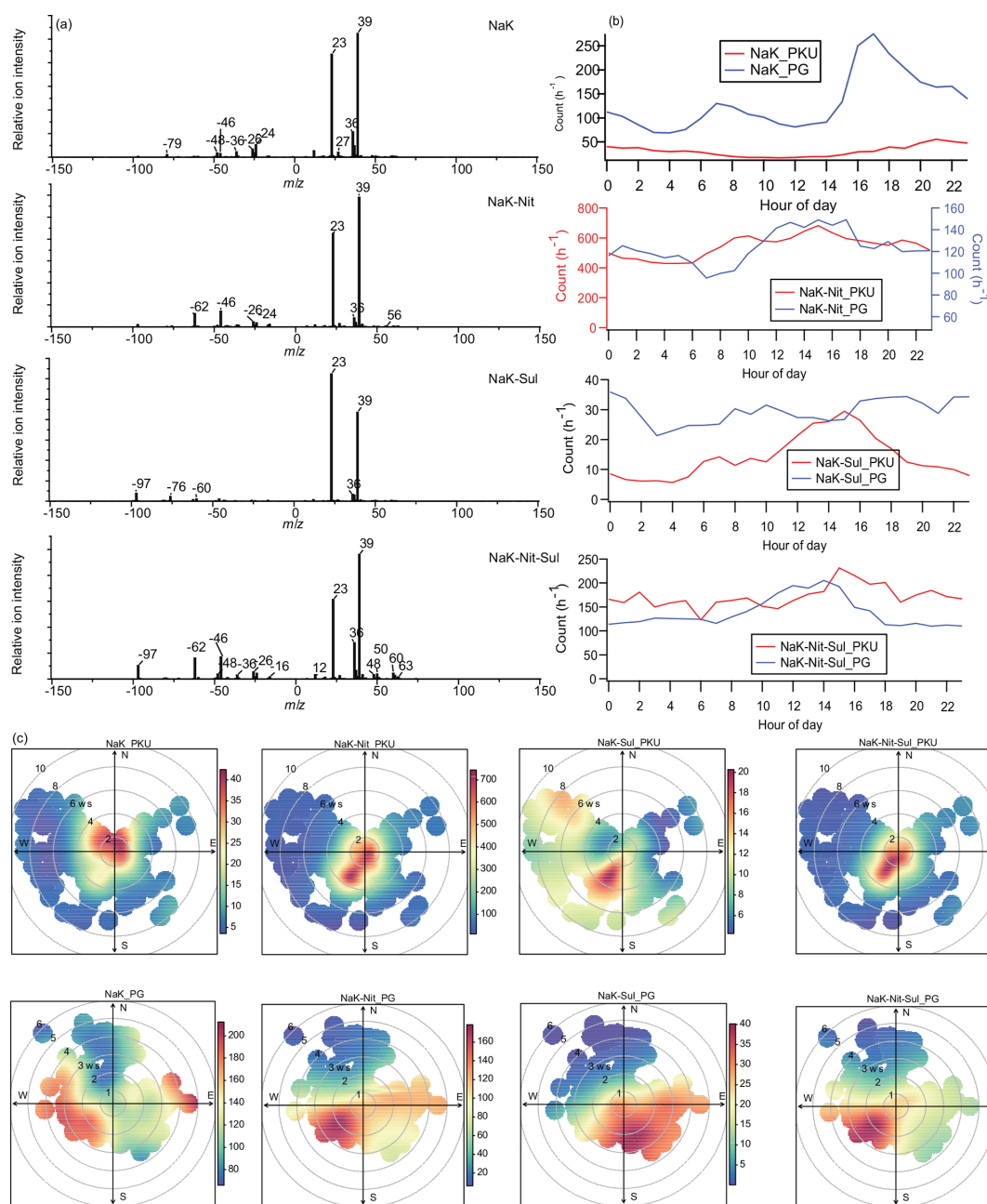


Figure 8. (a) Average mass spectra of NaK, NaK-Nit, NaK-Nit-Sul, and NaK-Sul observed at both sites; (b) diurnal patterns of the hourly count of NaK, NaK-Nit, NaK-Nit-Sul, and NaK-Sul at both sites; (c) polar plots of NaK, NaK-Nit, NaK-Nit-Sul, and NaK-Sul; the gray circles indicate wind speed (m s^{-1}).

(Xie et al., 2019). The processed particles, such as OC-Nit, ECOC-Nit, and NaK-Nit, were affected by emissions and secondary formations.

The emission and transport patterns were different in the urban and rural areas, resulting in different characteristics of PM. For example, EC particles were a key component at PKU (18.2% in total) but a minor particle type at PG (5.6%). Meanwhile, in the urban area of Beijing, direct emissions of K-rich particles should be small due to strict con-

trol measures; thus, the K-Nit-Sul particles are mainly from long-range transport. Transported particles were aged and commonly coated in a thick layer of nitrate and sulfate, but the local particles were affected by both emission and the near-surface aging process. For example, at PKU, the primary emission sources were traffic and central heating supply, causing an NO_x -rich region in which freshly emitted particle types could undergo processing due to the uptake of nitrate (Wang et al., 2016a). In the nearby villages of PG, do-

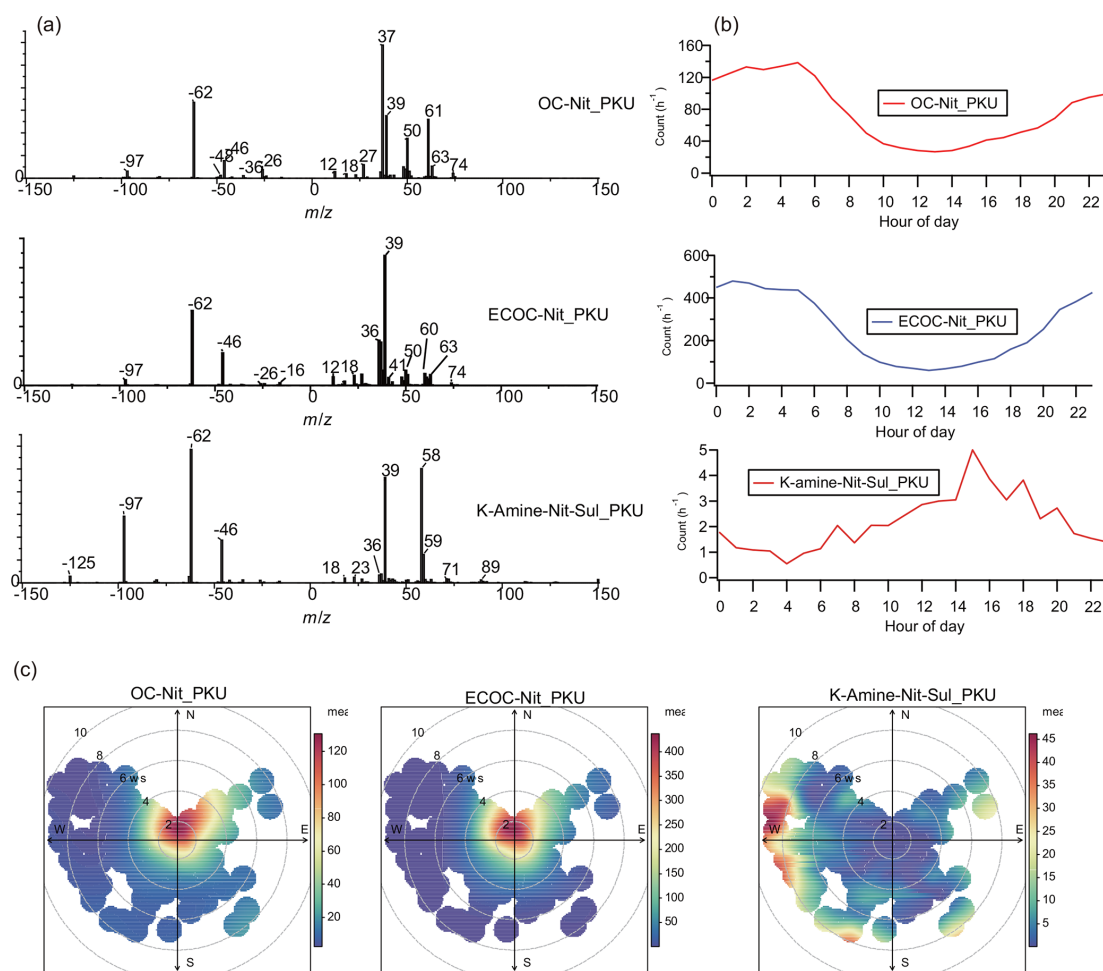


Figure 9. (a) Average mass spectra of OC-Nit_PKU, ECOC-Nit_PKU, and K-amine-Nit-Sul_PKU observed at the PKU site; (b) diurnal patterns of the hourly count of OC-Nit_PKU, ECOC-Nit_PKU, and K-amine-Nit-Sul_PKU at the PKU site; (c) polar plots of OC-Nit_PKU, ECOC-Nit_PKU, and K-amine-Nit-Sul_PKU; the gray circles indicate wind speed (m s^{-1}).

mestic heating and cooking were the major contributors of primary particles when the temperature was low in the morning and afternoon, resulting in the emission of multiple primary particle types such as OC_PG and ECOC_PG. In short, the characteristics of PM in urban and rural areas of Beijing were affected by local emissions, and they interacted with each other due to regional transport.

SO_2 was controlled strictly in Beijing. However, the emission of SO_2 is still significant in the nearby Hebei and Shandong provinces (Shi et al., 2019). The different control measures produced a low concentration area of SO_2 around Beijing. The sulfate-rich particle types, such as EC-Sul, OC-Sul, K-Sul, and NaK-Sul, arrived at the PKU site usually when wind speed was high ($> 3 \text{ m s}^{-1}$). The wind directions, along with the transport of sulfate-rich particles, were easterly, southwesterly, and southerly. In these directions, sulfate was primarily emitted from coal burning from residential heating, power generation, and industry, or there was secondary uptake on the preexisting particles (Zhang et al.,

2015). Likewise, a part of the sulfate-rich particles arrived at the PG site when wind speed was high. However, the locally formed particles were also pronounced, especially for ECOC-Sul, K-Sul, and NaK-Sul. As discussed in Sect. 3, ECOC-Sul and NaK-Sul were mainly from the coal burning for residential heating. The K-Sul was formed due to the uptake of secondary sulfate. Conclusively, the particulate characterization in rural areas around Beijing is influenced significantly by residential coal burning.

Secondary nitrate formation is still a critical issue in Beijing. The daytime rise in nitrate has been reported in studies (Sun et al., 2013), and we also found a similar predominance of nitrogen-containing particles in this study. Recent studies have reported the early morning peaks of nitrate using a soot particle aerosol mass spectrometer (SP-AMS) (Wang et al., 2019), which is consistent with our results. Interestingly, the early morning peak was only observed for several particle types at both sites, including EC-Nit_PKU, K-Nit_PKU, EC-Nit-Sul-PG, and EC-Nit_PG. This result is not surprising

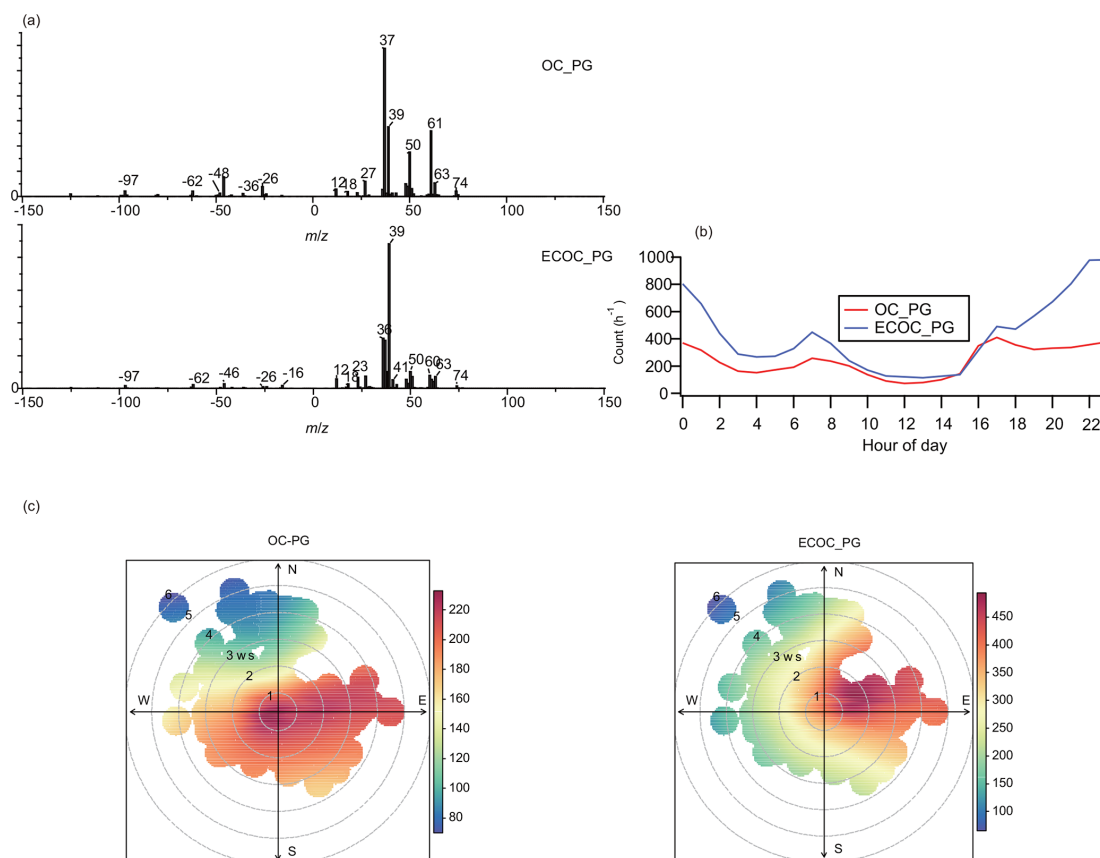


Figure 10. (a) Average mass spectra of OC_PG and ECOC_PG, (b) diurnal plots of OC_PG and ECOC_PG, and (c) polar plots of OC_PG and ECOC_PG. All these particle types appeared at the PG site.

because PG is also an NO_2 -rich region (Shi et al., 2019). The increasing contribution of nitrate-containing particles suggests the role of nighttime chemistry in nitrate uptake on particles. Wang et al. (2017) revealed the importance of nighttime N_2O_5 chemistry on nocturnal nitrate formation in the urban area of Beijing. The heterogeneous hydrolysis of N_2O_5 was most favorable when NO was at a low level. Moreover, the polar plots suggested a small role of long-range transport to the nitrate in individual particles. The contribution of local traffic was insignificant at the PG site as it was far from highways and major roads, the nighttime formation of nitrate appeared to be important in PG as well.

5 Conclusions

Two SPAMs were simultaneously deployed at urban and rural sites in Beijing in order to characterize PM during wintertime. The results at both sites indicate that they shared 17 types of common clusters, most of which belonged to particle categories such as EC, OC, ECOC, BB, and NaK. The origins and sources of these particle types at both sampling sites were also comprehensively analyzed. Most of the processed PM, including EC-Nit-Sul_PKU, ECOC-Nit-Sul_PKU, and

NaK-Nit-Sul_PKU, were aged locally in an NO_x -rich environment, while EC-Nit-Sul_PG, ECOC-Nit-Sul_PG, NaK-Nit-Sul_PG, and OC-Nit-Sul_PG were regional. Domestic heating in the rural area was found to be an important source of PM, and such heating activities typically caused three diurnal peaks in the early morning, morning, and afternoon (after sunset). Moreover, the early morning peak of nitrate was observed at both sites, suggesting the contribution of the heterogeneous hydrolysis of N_2O_5 in the dark during the winter. The insights gained in this study can provide useful references for understanding the relationship between regional transport and local aging in both urban and rural areas in Beijing. In Part 2, we focus on haze events observed at both sites and attempt to determine the effects of heating activities and possible regional transport between PKU and PG.

Data availability. All data described in this study are available upon request from the corresponding authors.

Author contributions. FY, MZ, TZ, QZ, and KH designed the experiments. YC, JC, ZW, MT, CP, and HY carried them out. XiY,

XiaY, YL, GS, and ZS analyzed the experimental data. YC prepared the article with contributions from all coauthors.

Competing interests. The authors declare that they have no conflict of interest.

Special issue statement. This article is part of the special issue “In-depth study of air pollution sources and processes within Beijing and its surrounding region (APHH-Beijing) (ACP/AMT inter-journal SI)”. It is not associated with a conference.

Acknowledgements. We are grateful for the financial support from the National Natural Science Foundation of China (grant nos. 4170030287 and 81571130100). Zongbo Shi is thankful for funding from NERC (NE/N007190/1 and NE/R005281/1).

Financial support. This research has been supported by the National Key Research and Development Programs of China (grant no. 2018YFC02004013) and the National Natural Science Foundation of China (grant nos. 41375123 and 81571130100).

Review statement. This article was edited by Frank Keutsch and reviewed by four anonymous referees.

References

- Bi, X., Zhang, G., Li, L., Wang, X., Li, M., Sheng, G., Fu, J., and Zhou, Z.: Mixing state of biomass burning particles by single particle aerosol mass spectrometer in the urban area of PRD, China, *Atmos. Environ.*, 45, 3447–3453, <https://doi.org/10.1016/j.atmosenv.2011.03.034>, 2011.
- Cai, J., Wang, J., Zhang, Y., Tian, H., Zhu, C., Gross, D. S., Hu, M., Hao, J., He, K., and Wang, S.: Source apportionment of Pb-containing particles in Beijing during January 2013, *Environ. Pollut.*, 226, 30–40, 2017.
- Chen, Y., Cao, J., Huang, R., Yang, F., Wang, Q., and Wang, Y.: Characterization, mixing state, and evolution of urban single particles in Xi’an (China) during wintertime haze days, *Sci. Total Environ.*, 573, 937–945, <https://doi.org/10.1016/j.scitotenv.2016.08.151>, 2016.
- Chen, Y., Wenger, J. C., Yang, F., Cao, J., Huang, R., Shi, G., Zhang, S., Tian, M., and Wang, H.: Source characterization of urban particles from meat smoking activities in Chongqing, China using single particle aerosol mass spectrometry, *Environ. Pollut.*, 228, 92–101, <https://doi.org/10.1016/j.envpol.2017.05.022>, 2017.
- Chen, Y., Tian, M., Huang, R.-J., Shi, G., Wang, H., Peng, C., Cao, J., Wang, Q., Zhang, S., Guo, D., Zhang, L., and Yang, F.: Characterization of urban amine-containing particles in south-western China: seasonal variation, source, and processing, *Atmos. Chem. Phys.*, 19, 3245–3255, <https://doi.org/10.5194/acp-19-3245-2019>, 2019.
- Chen, Y., Shi, G., Cai, J., Shi, Z., Wang, Z., Yao, X., Tian, M., Peng, C., Han, Y., Zhu, T., Liu, Y., Yang, X., Zheng, M., Yang, F., Zhang, Q., and He, K.: Simultaneous measurements of urban and rural particles in Beijing – Part 2: Case studies of haze events and regional transport, *Atmos. Chem. Phys.*, 20, 9249–9263, <https://doi.org/10.5194/acp-20-9249-2020>, 2020.
- Cheng, Y., Zheng, G., Wei, C., Mu, Q., Zheng, B., Wang, Z., Gao, M., Zhang, Q., He, K., and Carmichael, G.: Reactive nitrogen chemistry in aerosol water as a source of sulfate during haze events in China, *Sci. Adv.*, 2, e1601530, <https://doi.org/10.1126/sciadv.1601530>, 2016.
- Dalosto, M. and Harrison, R.: Chemical characterisation of single airborne particles in Athens (Greece) by ATOFMS, *Atmos. Environ.*, 40, 7614–7631, <https://doi.org/10.1016/j.atmosenv.2006.06.053>, 2006.
- Dall’Osto, M., Beddows, D., McGillicuddy, E. J., Esser-Gietl, J. K., Harrison, R. M., and Wenger, J. C.: On the simultaneous deployment of two single-particle mass spectrometers at an urban background and a roadside site during SAPUSS, *Atmos. Chem. Phys.*, 16, 9693–9710, 2016.
- Day, D. A., Liu, S., Russell, L. M., and Ziemann, P. J.: Organonitrate group concentrations in submicron particles with high nitrate and organic fractions in coastal southern California, *Atmos. Environ.*, 44, 1970–1979, <https://doi.org/10.1016/j.atmosenv.2010.02.045>, 2010.
- Du, W., Zhao, J., Wang, Y., Zhang, Y., Wang, Q., Xu, W., Chen, C., Han, T., Zhang, F., Li, Z., Fu, P., Li, J., Wang, Z., and Sun, Y.: Simultaneous measurements of particle number size distributions at ground level and 260 m on a meteorological tower in urban Beijing, China, *Atmos. Chem. Phys.*, 17, 6797–6811, <https://doi.org/10.5194/acp-17-6797-2017>, 2017.
- Gao, J., Zhang, Y., Zhang, M., Zhang, J., Wang, S., Tao, J., Wang, H., Luo, D., Chai, F., and Ren, C.: Photochemical properties and source of pollutants during continuous pollution episodes in Beijing, October, 2011, *J. Environ. Sci.-China*, 26, 44–53, [https://doi.org/10.1016/s1001-0742\(13\)60379-4](https://doi.org/10.1016/s1001-0742(13)60379-4), 2014.
- Gard, E., Mayer, J. E., Morrical, B. D., Dienes, T., Fergenson, D. P., and Prather, K. A.: Real-time analysis of individual atmospheric aerosol particles: Design and performance of a portable ATOFMS, *Anal. Chem.*, 69, 4083–4091, 1997.
- Ge, X., Wexler, A. S., and Clegg, S. L.: Atmospheric amines – Part I. A review, *Atmos. Environ.*, 45, 524–546, <https://doi.org/10.1016/j.atmosenv.2010.10.012>, 2011.
- Guo, S., Hu, M., Guo, Q., Zhang, X., Zheng, M., Zheng, J., Chang, C. C., Schauer, J. J., and Zhang, R.: Primary sources and secondary formation of organic aerosols in Beijing, China, *Environ. Sci. Technol.*, 46, 9846–9853, <https://doi.org/10.1021/es2042564>, 2012.
- Guo, S., Hu, M., Zamora, M. L., Peng, J., Shang, D., Zheng, J., Du, Z., Wu, Z., Shao, M., Zeng, L., Molina, M. J., and Zhang, R.: Elucidating severe urban haze formation in China, *P. Natl. Acad. Sci. USA*, 111, 17373–17378, <https://doi.org/10.1073/pnas.1419604111>, 2014.
- He, K., Yang, F., Ma, Y., Zhang, Q., Yao, X., Chan, C. K., Cadle, S., Chan, T., and Mulawa, P.: The characteristics of PM_{2.5} in Beijing, China, *Atmos. Environ.*, 35, 4959–4970, [https://doi.org/10.1016/s1352-2310\(01\)00301-6](https://doi.org/10.1016/s1352-2310(01)00301-6), 2001.
- Healy, R. M., Hellebust, S., Kourtchev, I., Allanic, A., O’Connor, I. P., Bell, J. M., Healy, D. A., Sodeau, J. R., and Wenger, J. C.:

- Source apportionment of PM_{2.5} in Cork Harbour, Ireland using a combination of single particle mass spectrometry and quantitative semi-continuous measurements, *Atmos. Chem. Phys.*, 10, 9593–9613, <https://doi.org/10.5194/acp-10-9593-2010>, 2010.
- Healy, R. M., Sciare, J., Poulain, L., Kamili, K., Merkel, M., Müller, T., Wiedensohler, A., Eckhardt, S., Stohl, A., Sarda-Estève, R., McGillicuddy, E., O'Connor, I. P., Sodeau, J. R., and Wenger, J. C.: Sources and mixing state of size-resolved elemental carbon particles in a European megacity: Paris, *Atmos. Chem. Phys.*, 12, 1681–1700, <https://doi.org/10.5194/acp-12-1681-2012>, 2012.
- Huang, M., Hao, L., Guo, X., Hu, C., Gu, X., Zhao, W., Wang, Z., Fang, L., and Zhang, W.: Characterization of secondary organic aerosol particles using aerosol laser time-of-flight mass spectrometer coupled with FCM clustering algorithm, *Atmos. Environ.*, 64, 85–94, <https://doi.org/10.1016/j.atmosenv.2012.09.044>, 2013.
- Huang, R. J., Zhang, Y., Bozzetti, C., Ho, K. F., Cao, J. J., Han, Y., Daellenbach, K. R., Slowik, J. G., Platt, S. M., Canonaco, F., Zotter, P., Wolf, R., Pieber, S. M., Bruns, E. A., Crippa, M., Ciarelli, G., Piazzalunga, A., Schwikowski, M., Abbaszade, G., Schnelle-Kreis, J., Zimmermann, R., An, Z., Szidat, S., Baltensperger, U., El Haddad, I., and Prevot, A. S.: High secondary aerosol contribution to particulate pollution during haze events in China, *Nature*, 514, 218–222, <https://doi.org/10.1038/nature13774>, 2014.
- Huang, X.-F., He, L.-Y., Hu, M., and Zhang, Y.-H.: Annual variation of particulate organic compounds in PM_{2.5} in the urban atmosphere of Beijing, *Atmos. Environ.*, 40, 2449–2458, <https://doi.org/10.1016/j.atmosenv.2005.12.039>, 2006.
- Huang, X.-F., He, L.-Y., Hu, M., Canagaratna, M. R., Sun, Y., Zhang, Q., Zhu, T., Xue, L., Zeng, L.-W., Liu, X.-G., Zhang, Y.-H., Jayne, J. T., Ng, N. L., and Worsnop, D. R.: Highly time-resolved chemical characterization of atmospheric submicron particles during 2008 Beijing Olympic Games using an Aerodyne High-Resolution Aerosol Mass Spectrometer, *Atmos. Chem. Phys.*, 10, 8933–8945, <https://doi.org/10.5194/acp-10-8933-2010>, 2010.
- Li, L., Huang, Z., Dong, J., Li, M., Gao, W., Nian, H., Fu, Z., Zhang, G., Bi, X., Cheng, P., and Zhou, Z.: Real time bipolar time-of-flight mass spectrometer for analyzing single aerosol particles, *Int. J. Mass Spectrom.*, 303, 118–124, <https://doi.org/10.1016/j.ijms.2011.01.017>, 2011.
- Li, L., Li, M., Huang, Z., Gao, W., Nian, H., Fu, Z., Gao, J., Chai, F., and Zhou, Z.: Ambient particle characterization by single particle aerosol mass spectrometry in an urban area of Beijing, *Atmos. Environ.*, 94, 323–331, <https://doi.org/10.1016/j.atmosenv.2014.03.048>, 2014.
- Li, P., Yan, R., Yu, S., Wang, S., Liu, W., and Bao, H.: Reinstatement regional transport of PM_{2.5} as a major cause of severe haze in Beijing, *P. Natl. Acad. Sci. USA*, 112, E2739–2740, <https://doi.org/10.1073/pnas.1502596112>, 2015a.
- Li, P., Yan, R., Yu, S., Wang, S., Liu, W., and Bao, H.: Reinstatement regional transport of PM_{2.5} as a major cause of severe haze in Beijing, *P. Natl. Acad. Sci. USA*, 112, E2739–E2740, <https://doi.org/10.1073/pnas.1502596112>, 2015b.
- Liu, D., Joshi, R., Wang, J., Yu, C., Allan, J. D., Coe, H., Flynn, M. J., Xie, C., Lee, J., Squires, F., Kotthaus, S., Grimmond, S., Ge, X., Sun, Y., and Fu, P.: Contrasting physical properties of black carbon in urban Beijing between winter and summer, *Atmos. Chem. Phys.*, 19, 6749–6769, <https://doi.org/10.5194/acp-19-6749-2019>, 2019.
- Liu, J., Mauzerall, D. L., Chen, Q., Zhang, Q., Song, Y., Peng, W., Klimont, Z., Qiu, X., Zhang, S., Hu, M., Lin, W., Smith, K. R., and Zhu, T.: Air pollutant emissions from Chinese households: A major and underappreciated ambient pollution source, *P. Natl. Acad. Sci. USA*, 113, 7756–7761, <https://doi.org/10.1073/pnas.1604537113>, 2016.
- Liu, L., Wang, Y., Du, S., Zhang, W., Hou, L., Vedral, S., Han, B., Yang, W., Chen, M., and Bai, Z.: Characteristics of atmospheric single particles during haze periods in a typical urban area of Beijing: A case study in October, 2014, *J. Environ. Sci.-China*, 40, 145–153, <https://doi.org/10.1016/j.jes.2015.10.027>, 2016.
- Liu, Y., Zheng, M., Yu, M., Cai, X., Du, H., Li, J., Zhou, T., Yan, C., Wang, X., Shi, Z., Harrison, R. M., Zhang, Q., and He, K.: High-time-resolution source apportionment of PM_{2.5} in Beijing with multiple models *Atmos. Chem. Phys. Discuss.*, <https://doi.org/10.5194/acp-2018-1234>, 2018.
- Liu, Y., Zheng, M., Yu, M., Cai, X., Du, H., Li, J., Zhou, T., Yan, C., Wang, X., Shi, Z., Harrison, R. M., Zhang, Q., and He, K.: High-time-resolution source apportionment of PM_{2.5} in Beijing with multiple models, *Atmos. Chem. Phys.*, 19, 6595–6609, <https://doi.org/10.5194/acp-19-6595-2019>, 2019.
- Ma, L., Li, M., Huang, Z., Li, L., Gao, W., Nian, H., Zou, L., Fu, Z., Gao, J., Chai, F., and Zhou, Z.: Real time analysis of lead-containing atmospheric particles in Beijing during springtime by single particle aerosol mass spectrometry, *Chemosphere*, 154, 454–462, <https://doi.org/10.1016/j.chemosphere.2016.04.001>, 2016.
- McGuire, M. L., Jeong, C.-H., Slowik, J. G., Chang, R. Y.-W., Corbin, J. C., Lu, G., Mihele, C., Rehbein, P. J. G., Sills, D. M. L., Abbatt, J. P. D., Brook, J. R., and Evans, G. J.: Elucidating determinants of aerosol composition through particle-type-based receptor modeling, *Atmos. Chem. Phys.*, 11, 8133–8155, <https://doi.org/10.5194/acp-11-8133-2011>, 2011.
- Pagels, J., Dutcher, D. D., Stolzenburg, M. R., McMurry, P. H., Gälli, M. E., and Gross, D. S.: Fine-particle emissions from solid biofuel combustion studied with single-particle mass spectrometry: Identification of markers for organics, soot, and ash components, *J. Geophys. Res.-Atmos.*, 118, 859–870, <https://doi.org/10.1029/2012jd018389>, 2013.
- Peng, C., Tian, M., Wang, X., Yang, F., Shi, G., Huang, R.-J., Yao, X., Wang, Q., Zhai, C., Zhang, S., Qian, R., Cao, J., and Chen, Y.: Light absorption of brown carbon in PM_{2.5} in the Three Gorges Reservoir region, southwestern China: Implications of biomass burning and secondary formation, *Atmos. Environ.*, 229, 117409, <https://doi.org/10.1016/j.atmosenv.2020.117409>, 2020a.
- Peng, C., Yang, F., Tian, M., Shi, G., Li, L., Huang, R. J., Yao, X., Luo, B., Zhai, C., and Chen, Y.: Brown carbon aerosol in two megacities in the Sichuan Basin of southwestern China: Light absorption properties and implications, *Sci. Total Environ.*, 719, 137483, <https://doi.org/10.1016/j.scitotenv.2020.137483>, 2020b.
- Pratt, K. A. and Prather, K. A.: Mass spectrometry of atmospheric aerosols—recent developments and applications. Part 2: On-line mass spectrometry techniques, *Mass Spectrom. Rev.*, 31, 17–48, <https://doi.org/10.1002/mas.20330>, 2012.
- Qin, X., Pratt, K. A., Shields, L. G., Toner, S. M., and Prather, K. A.: Seasonal comparisons of single-particle chemical mix-

- ing state in Riverside, CA, *Atmos. Environ.*, 59, 587–596, <https://doi.org/10.1016/j.atmosenv.2012.05.032>, 2012.
- Shi, Z., Vu, T., Kotthaus, S., Harrison, R. M., Grimmond, S., Yue, S., Zhu, T., Lee, J., Han, Y., Demuzere, M., Dunmore, R. E., Ren, L., Liu, D., Wang, Y., Wild, O., Allan, J., Acton, W. J., Barlow, J., Barratt, B., Beddows, D., Bloss, W. J., Calzolari, G., Carruthers, D., Carslaw, D. C., Chan, Q., Chatzidiakou, L., Chen, Y., Crilley, L., Coe, H., Dai, T., Doherty, R., Duan, F., Fu, P., Ge, B., Ge, M., Guan, D., Hamilton, J. F., He, K., Heal, M., Heard, D., Hewitt, C. N., Hollaway, M., Hu, M., Ji, D., Jiang, X., Jones, R., Kalberer, M., Kelly, F. J., Kramer, L., Langford, B., Lin, C., Lewis, A. C., Li, J., Li, W., Liu, H., Liu, J., Loh, M., Lu, K., Lucarelli, F., Mann, G., McFiggans, G., Miller, M. R., Mills, G., Monk, P., Nemitz, E., O'Connor, F., Ouyang, B., Palmer, P. I., Percival, C., Popoola, O., Reeves, C., Rickard, A. R., Shao, L., Shi, G., Spracklen, D., Stevenson, D., Sun, Y., Sun, Z., Tao, S., Tong, S., Wang, Q., Wang, W., Wang, X., Wang, X., Wang, Z., Wei, L., Whalley, L., Wu, X., Wu, Z., Xie, P., Yang, F., Zhang, Q., Zhang, Y., Zhang, Y., and Zheng, M.: Introduction to the special issue “In-depth study of air pollution sources and processes within Beijing and its surrounding region (APHH-Beijing)”, *Atmos. Chem. Phys.*, 19, 7519–7546, <https://doi.org/10.5194/acp-19-7519-2019>, 2019.
- Silva, P. J., Liu, D.-Y., Noble, C. A., and Prather, K. A.: Size and Chemical Characterization of Individual Particles Resulting from Biomass Burning of Local Southern California Species, *Environ. Sci. Technol.*, 33, 3068–3076, <https://doi.org/10.1021/es980544p>, 1999.
- Silva, P. J., Carlin, R. A., and Prather, K. A.: Single particle analysis of suspended soil dust from Southern California, *Atmos. Environ.*, 34, 1811–1820, [https://doi.org/10.1016/S1352-2310\(99\)00338-6](https://doi.org/10.1016/S1352-2310(99)00338-6), 2000.
- Sodeman, D. A., Toner, S. M., and Prather, K. A.: Determination of single particle mass spectral signatures from light-duty vehicle emissions, *Environ. Sci. Technol.*, 39, 4569–4580, <https://doi.org/10.1021/es0489947>, 2005.
- Song, X. H., Hopke, P. K., Fergenson, D. P., and Prather, K. A.: Classification of single particles analyzed by ATOFMS using an artificial neural network, ART-2A, *Anal. Chem.*, 71, 860–865, <https://doi.org/10.1021/ac9809682>, 1999.
- Sullivan, R. C., Guazzotti, S. A., Sodeman, D. A., Tang, Y., Carmichael, G. R., and Prather, K. A.: Mineral dust is a sink for chlorine in the marine boundary layer, *Atmos. Environ.*, 41, 7166–7179, <https://doi.org/10.1016/j.atmosenv.2007.05.047>, 2007.
- Sun, Y., Jiang, Q., Wang, Z., Fu, P., Li, J., Yang, T., and Yin, Y.: Investigation of the sources and evolution processes of severe haze pollution in Beijing in January 2013, *J. Geophys. Res.*, 119, 4380–4398, 2014a.
- Sun, Y., Jiang, Q., Wang, Z., Fu, P., Li, J., Yang, T., and Yin, Y.: Investigation of the sources and evolution processes of severe haze pollution in Beijing in January 2013, *J. Geophys. Res.-Atmos.*, 119, 4380–4398, <https://doi.org/10.1002/2014jd021641>, 2014b.
- Sun, Y. L., Wang, Z. F., Fu, P. Q., Yang, T., Jiang, Q., Dong, H. B., Li, J., and Jia, J. J.: Aerosol composition, sources and processes during wintertime in Beijing, China, *Atmos. Chem. Phys.*, 13, 4577–4592, <https://doi.org/10.5194/acp-13-4577-2013>, 2013.
- Tao, S., Wang, X., Chen, H., Yang, X., Li, M., Li, L., and Zhou, Z.: Single particle analysis of ambient aerosols in Shanghai during the World Exposition, 2010: two case studies, *Front. Environ. Sci. En.*, 5, 391–401, <https://doi.org/10.1007/s11783-011-0355-x>, 2011.
- Toner, S. M., Sodeman, D. A., and Prather, K. A.: Single particle characterization of ultrafine and accumulation mode particles from heavy duty diesel vehicles using aerosol time-of-flight mass spectrometry, *Environ. Sci. Technol.*, 40, 3912–3921, 2006.
- Toner, S. M., Shields, L. G., Sodeman, D. A., and Prather, K. A.: Using mass spectral source signatures to apportion exhaust particles from gasoline and diesel powered vehicles in a free-way study using UF-ATOFMS, *Atmos. Environ.*, 42, 568–581, <https://doi.org/10.1016/j.atmosenv.2007.08.005>, 2008.
- Wang, G., Zhang, R., Gomez, M. E., Yang, L., Levy Zamora, M., Hu, M., Lin, Y., Peng, J., Guo, S., Meng, J., Li, J., Cheng, C., Hu, T., Ren, Y., Wang, Y., Gao, J., Cao, J., An, Z., Zhou, W., Li, G., Wang, J., Tian, P., Marrero-Ortiz, W., Secret, J., Du, Z., Zheng, J., Shang, D., Zeng, L., Shao, M., Wang, W., Huang, Y., Wang, Y., Zhu, Y., Li, Y., Hu, J., Pan, B., Cai, L., Cheng, Y., Ji, Y., Zhang, F., Rosenfeld, D., Liss, P. S., Duce, R. A., Kolb, C. E., and Molina, M. J.: Persistent sulfate formation from London Fog to Chinese haze, *P. Natl. Acad. Sci. USA*, 113, 13630–13635, <https://doi.org/10.1073/pnas.1616540113>, 2016a.
- Wang, G., Zhang, R., Gomez, M. E., Yang, L., Zamora, M. L., Hu, M., Lin, Y., Peng, J., Guo, S., and Meng, J.: Persistent sulfate formation from London Fog to Chinese haze, *P. Natl. Acad. Sci. USA*, 113, 13630–13635, 2016b.
- Wang, H., Zhu, B., Zhang, Z., An, J., and Shen, L.: Mixing state of individual carbonaceous particles during a severe haze episode in January 2013, Nanjing, China, *Particology*, 20, 16–23, <https://doi.org/10.1016/j.partic.2014.06.013>, 2015.
- Wang, H., Lu, K., Chen, X., Zhu, Q., Chen, Q., Guo, S., Jiang, M., Li, X., Shang, D., Tan, Z., Wu, Y., Wu, Z., Zou, Q., Zheng, Y., Zeng, L., Zhu, T., Hu, M., and Zhang, Y.: High N₂O₅ Concentrations Observed in Urban Beijing: Implications of a Large Nitrate Formation Pathway, *Environ. Sci. Technol. Lett.*, 4, 416–420, <https://doi.org/10.1021/acs.estlett.7b00341>, 2017.
- Wang, J., Liu, D., Ge, X., Wu, Y., Shen, F., Chen, M., Zhao, J., Xie, C., Wang, Q., Xu, W., Zhang, J., Hu, J., Allan, J., Joshi, R., Fu, P., Coe, H., and Sun, Y.: Characterization of black carbon-containing fine particles in Beijing during wintertime, *Atmos. Chem. Phys.*, 19, 447–458, <https://doi.org/10.5194/acp-19-447-2019>, 2019.
- Wang, P., Pan, B., Li, H., Huang, Y., Dong, X., Ai, F., Liu, L., Wu, M., and Xing, B.: The Overlooked Occurrence of Environmentally Persistent Free Radicals in an Area with Low-Rank Coal Burning, Xuanwei, China, *Environ. Sci. Technol.*, 52, 1054–1061, <https://doi.org/10.1021/acs.est.7b05453>, 2018.
- Xie, C., Xu, W., Wang, J., Wang, Q., Liu, D., Tang, G., Chen, P., Du, W., Zhao, J., Zhang, Y., Zhou, W., Han, T., Bian, Q., Li, J., Fu, P., Wang, Z., Ge, X., Allan, J., Coe, H., and Sun, Y.: Vertical characterization of aerosol optical properties and brown carbon in winter in urban Beijing, China, *Atmos. Chem. Phys.*, 19, 165–179, <https://doi.org/10.5194/acp-19-165-2019>, 2019.
- Xu, J., Li, M., Shi, G., Wang, H., Ma, X., Wu, J., Shi, X., and Feng, Y.: Mass spectra features of biomass burning boiler and coal burning boiler emitted particles by single particle aerosol mass spectrometer, *Sci. Total Environ.*, 598, 341–352, <https://doi.org/10.1016/j.scitotenv.2017.04.132>, 2017.

- Xu, J., Wang, H., Li, X., Li, Y., Wen, J., Zhang, J., Shi, X., Li, M., Wang, W., Shi, G., and Feng, Y.: Refined source apportionment of coal combustion sources by using single particle mass spectrometry, *Sci. Total Environ.*, 627, 633–646, <https://doi.org/10.1016/j.scitotenv.2018.01.269>, 2018.
- Xu, W. Q., Sun, Y. L., Chen, C., Du, W., Han, T. T., Wang, Q. Q., Fu, P. Q., Wang, Z. F., Zhao, X. J., Zhou, L. B., Ji, D. S., Wang, P. C., and Worsnop, D. R.: Aerosol composition, oxidation properties, and sources in Beijing: results from the 2014 Asia-Pacific Economic Cooperation summit study, *Atmos. Chem. Phys.*, 15, 13681–13698, <https://doi.org/10.5194/acp-15-13681-2015>, 2015.
- Zhai, J., Wang, X., Li, J., Xu, T., Chen, H., Yang, X., and Chen, J.: Thermal desorption single particle mass spectrometry of ambient aerosol in Shanghai, *Atmos. Environ.*, 123, 407–414, <https://doi.org/10.1016/j.atmosenv.2015.09.001>, 2015.
- Zhai, S., An, X., Zhao, T., Sun, Z., Wang, W., Hou, Q., Guo, Z., and Wang, C.: Detection of critical PM_{2.5} emission sources and their contributions to a heavy haze episode in Beijing, China, using an adjoint model, *Atmos. Chem. Phys.*, 18, 6241–6258, <https://doi.org/10.5194/acp-18-6241-2018>, 2018.
- Zhang, R., Wang, G., Guo, S., Zamora, M. L., Ying, Q., Lin, Y., Wang, W., Hu, M., and Wang, Y.: Formation of urban fine particulate matter, *Chem. Rev.*, 115, 3803–3855, <https://doi.org/10.1021/acs.chemrev.5b00067>, 2015.
- Zhao, J., Qiu, Y., Zhou, W., Xu, W., Wang, J., Zhang, Y., Li, L., Xie, C., Wang, Q., Du, W., Worsnop, D. R., Canagaratna, M. R., Zhou, L., Ge, X., Fu, P., Li, J., Wang, Z., Donahue, N. M., and Sun, Y.: Organic Aerosol Processing During Winter Severe Haze Episodes in Beijing, *J. Geophys. Res.-Atmos.*, 124, 10248–10263, <https://doi.org/10.1029/2019JD030832>, 2019.
- Zheng, M., Yan, C. Q., Wang, S. X., He, K. B., and Zhang, Y. H.: Understanding PM_{2.5} sources in China: challenges and perspectives, *Natl. Sci. Rev.*, 4, 801–803, <https://doi.org/10.1093/nsr/nwx129>, 2017.
- Zou, Y., Deng, X. J., Zhu, D., Gong, D. C., Wang, H., Li, F., Tan, H. B., Deng, T., Mai, B. R., Liu, X. T., and Wang, B. G.: Characteristics of 1 year of observational data of VOCs, NO_x and O₃ at a suburban site in Guangzhou, China, *Atmos. Chem. Phys.*, 15, 6625–6636, <https://doi.org/10.5194/acp-15-6625-2015>, 2015.